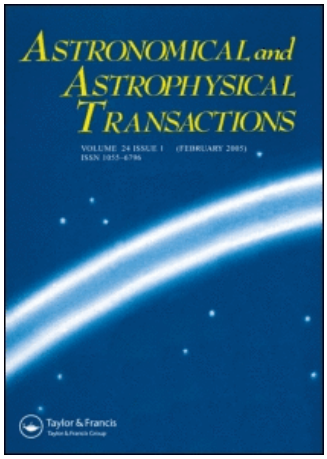


Astronomical & Astrophysical Transactions
The Journal of the Eurasian Astronomical Society
Publication details, including instructions for authors and subscription information:
http://www.informaworld.com/smpp/title~content=t713453505

# Orbits in global and local galactic potentials

N. D. Caranicolas [a]
[a] Department of Physics, Section of Astrophysics, Astronomy and Mechanics, University of Thessaloniki, Thessaloniki, Greece

Online Publication Date: 01 June 2004
To cite this Article: Caranicolas, N. D. (2004) 'Orbits in global and local galactic potentials', Astronomical & Astrophysical Transactions, 23:3, 241 - 252
To link to this article: DOI: 10.1080/10556790410001704668
URL: http://dx.doi.org/10.1080/10556790410001704668

*Astronomical and Astrophysical Transactions*
Vol. 23, No. 3, June 2004, pp. 241–252

Taylor & Francis
Taylor & Francis Group



# ORBITS IN GLOBAL AND LOCAL GALACTIC POTENTIALS

N. D. CARANICOLAS*

*Department of Physics, Section of Astrophysics, Astronomy and Mechanics, University of Thessaloniki, 540 06 Thessaloniki, Greece*

*(Received 27 May 2003)*

Connections between global and local potentials in two galactic models are described. The first model is a logarithmic potential while the second is a four-component mass model. The first model describes plane motion in an elliptical galaxy with a dense nucleus or bulge of radius $c$, while the second is a composite mass model. Expanding the global potentials in the vicinity of a circular orbit, we find the potential of the corresponding two-dimensional perturbed harmonic oscillator. In the first case, the local potential shows two interesting resonances: the 1:1 and the 4:3 resonances. The appearance of these two cases depends on the flattening parameter of the global potential or the position of the equilibrium point. Expressions connecting the parameters of the global and local potentials are obtained. The second model produces a local potential that can show a large number of resonances depending on the position of the equilibrium point. A relation between the global and local energies of the system is given in both cases.

*Keywords*: Orbits; Global potential; Local potential; Galactic models

## 1 INTRODUCTION

It is well known in galactic dynamics that, to first order, local motion in a galaxy model can be described by a two-dimensional perturbed harmonic oscillator potential

$$V(x, y) = \tfrac{1}{2}(\omega_1^2 x^2 + \omega_2^2 y^2) + \epsilon V_1, \tag{1}$$

where $\omega_1$ and $\omega_2$ are the unperturbed frequencies of oscillation along the $x$ and $y$-axes respectively, $\epsilon$ is the perturbation strength, while $V_1$ is a polynomial containing the perturbing terms. Furthermore, we note that the form of the potential (1) is not arbitrary but comes from the expansion of potentials, relevant for actual galaxies, near an equilibrium point (*i.e.* a circular orbit). This means that the parameters entering equation (1) are not arbitrary but can be connected to the physical quantities of the global system. Note that, in order to obtain the potential (1) for the local motion, we must have a time-independent three-dimensional global potential describing motion in a galaxy with an axis and a plane of symmetry. This means that the potential, in cylindrical coordinates, must be of the form $V = V(r, z^2)$ (Binney and Tremaine, 1987, p. 121).

* E-mail: caranic@astro.auth.gr

ISSN 1055-6796 print; ISSN 1476-3540 online 
DOI: 10.1080/10556790410001704668

In this work, connections between global and local potentials are described. The motivation for this work is as follows.

(i) It is useful to find relations between global physical quantities such as energy, angular momentum or flattering, and local physical quantities such as energy, local resonances and local zero-velocity curves. Therefore it is of interest to observe the differences in the local parameters as the physical quantities of the global system change.
(ii) As the local system has a polynomial form, it is simple, and it is possible to find analytical expressions describing the local physical or dynamic properties. For instance, it is easy to find analytical expressions for a potential of the form (1) using action angle variables (Caranicolas, 1989, 1990). Furthermore, it would be interesting to follow the evolution of these analytical expressions as the physical parameters of the global system change.
(iii) It is also important to make a comparison between the characteristics of orbits of the global and local systems. This comparison could be considered as a first step of study, in future work, the effects on local motions of important features in the interior of our Galaxy, such as a central bar or a non-axisymmetric spheroidal mass.

In the present paper we employ, as one of the global models, the logarithmic potential

$$U(r, z) = \tfrac{1}{2} \ln(r^2 + \alpha z^2 + c^2), \tag{2}$$

where $r$ and $z$ are the usual cylindrical coordinates while $\alpha$ and $c$ are parameters. Potential (2) is important for galactic dynamics and represents an elliptical galaxy with a nucleus or bulge of scale size $c$, which displays a flat rotation curve at large radii (Binney and Tremaine, 1987). The parameter $1 < \alpha < 2$ defines the axial ratio of the equipotential ellipsoids. It is important to note that the equipotential curves in the $(r, z)$ plane are only a third as flattened as the contours of equal density, and the density becomes negative on the $z$ axis when $\alpha > 2$. Logarithmic potentials have been frequently used by many investigators, in order to model galactic motion (see for example Richstone (1980, 1982) and Caranicolas and Vozikis (1986)).

The properties of the global motion in the potential (2) have been studied in a recent paper (Karanis and Caranicolas, 2001). The primary aim of the present work is to study the properties of the local potential (1) arising from the dynamic model (2). In particular, we shall find the connection of the parameters of the potential (1) with the physical quantities $\alpha$ and $c$. Of special interest are the possible local resonance cases: When $\omega_1/\omega_2$ is close to a rational number $q = n/m$. Furthermore, we wish to find a relation between the global and local energies. The derivation of the local potential and a connection between global and local parameters are given in Section 2. In Section 3 we study the properties of global motion and local motion in the resonance cases. A discussion and conclusions are given in Section 4.

## 2 CHARACTERISTICS OF THE LOCAL POTENTIAL

The Hamiltonian of the potential (2) is

$$H_{\mathrm{G}} = \tfrac{1}{2}\left(p_r^2 + p_z^2 + \frac{L_z^2}{2r^2}\right) + U(r, z) = \tfrac{1}{2}(p_r^2 + p_z^2) + V_{\mathrm{eff}}(r, z) = E, \tag{3}$$

where $p_r$ and $p_z$ are the momenta per unit mass conjugate to $r$ and $z$, $L_z$ is the angular momentum and $E$ is the numerical value of $H$. The potential $V_{\mathrm{eff}} = L_z^2/2r^2 + U(r, z)$, describing the motion in the $(r, z)$ plane, is called the effective potential.

The local potential can be found by expanding the effective potential in the vicinity of a circular orbit ($r = r_0$, $z = 0$). Thus we have

$$V_{\rm eff}(r_0 + \Delta r, \Delta z) = V_{\rm eff}(r_0, 0) + \tfrac{1}{2}A(\Delta r)^2 + \tfrac{1}{2}B(\Delta z)^2 + [\alpha_1 \Delta r(\Delta z)^2 + \alpha_2(\Delta r)^3 + \cdots], \tag{4}$$

where

$$\begin{aligned} A &= \frac{3L_z^2}{r_0^4} + \left(\frac{\partial^2 U}{\partial r^2}\right)_{r_0,0}, \\ B &= \left(\frac{\partial^2 U}{\partial z^2}\right)_{r_0,0}, \\ \alpha_1 &= \frac{1}{2}\left(\frac{\partial^2 U}{\partial r \partial z}\right)_{r_0,0}, \\ \alpha_2 &= -\frac{2L_z^2}{r_0^5} + \frac{1}{6}\left(\frac{\partial^3 U}{\partial r^3}\right)_{r_0,0}, \end{aligned} \tag{5}$$

and we have taken into account the condition for the circular orbit as well as the fact $V_{\rm eff}$ is symmetric about $z = 0$. Dividing both sides of equation (4) by $A$ and writing $V = [V_{\rm eff}(r_0 + \Delta r, \Delta z) - V_{\rm eff}(r_0, 0)]/A$, $B/A = \omega^2$, $\beta = \alpha_1/A$, $\gamma = \alpha_2/A$, $x = \Delta r$ and $y = \Delta z$, we obtain

$$V(x, y) = \tfrac{1}{2}(x^2 + \omega^2 y^2) + \beta x y^2 + \gamma x^3, \tag{6}$$

which is the local potential. In this potential, only third-order terms in the variables have been retained. The following arguments justify our choice.

(i) This potential has been used by many investigators in order to study local motion in galaxies or the properties of nonlinear harmonic oscillators, for more than three decades (see for example Henon and Heiles (1964), Saito and Ichimura (1974), Innanen (1985) and Elipe *et al*. (1995)).
(ii) In spite of its simplicity, it is characterized by interesting resonance phenomena and large chaotic regions for certain values of the parameters $\omega$, $\beta$ and $\gamma$.

Figure 1 shows a plot of the ratio $q = 1/\omega$ as a function of the flattening parameter $\alpha$ when the position of the circular orbit is at $r_0 = 0.6$. We see that the system can come close to the 1:1 and the 4:3 resonance cases. One notes that a change in the value of the scale size of the nucleus $c$ does not affect drastically the appearance of the above resonances. In Figure 2, $q$ is shown as a function of the position $r_0$ of the circular orbit, when $\alpha = 2$. Here the situation appears different. One observes that the system can show phenomena connected with two resonance cases, that is the 1:1 and the 4:3 cases, only when $c = 0.15$. For a dense nucleus with $c = 0.01$, the system stays close to the 1:1 resonance.

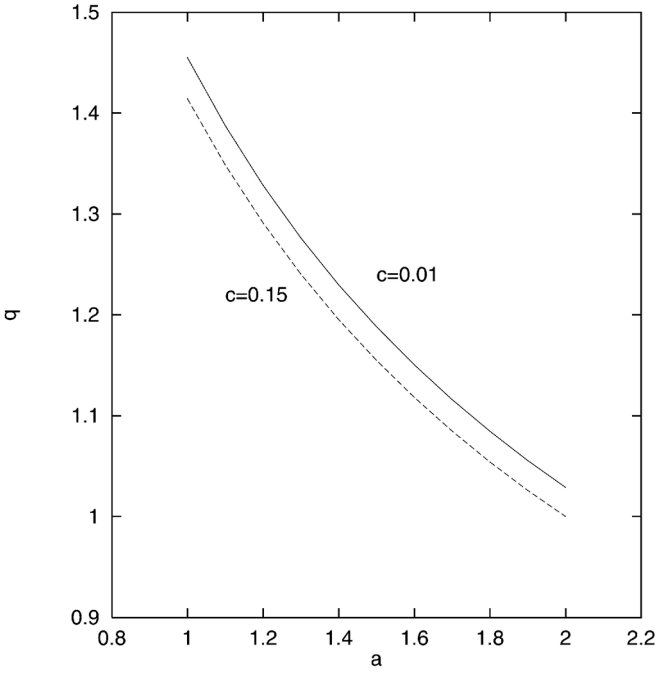


FIGURE 1 Relationship between $q$ and the flattening parameter $\alpha$ in the local expansion of the logarithmic potential for two values of $c$. Note that the system shows similar behaviours for both values of $c$.

The above behaviour can be explained using the analytical expressions for $q$. In the following we give the expressions for the parameters $q, \beta$ and $\gamma$ with respect to $\alpha$ and $c$. These expressions are

$$
\begin{aligned}
A &= \frac{3L_z^2}{r_0^4} + \frac{c^2 - r_0^2}{(c^2 + r_0^2)^2}, \\
B &= \frac{\alpha}{c^2 + r_0^2}, \\
q &= \left[ \frac{c^2 + r_0^2}{\alpha} \left( \frac{3L_z^2}{r_0^4} + \frac{c^2 - r_0^2}{(c^2 + r_0^2)^2} \right) \right]^{1/2}, \\
\beta &= \frac{-\alpha r_0}{(c^2 + r_0^2)^2 \left[ 3L_z^2/r_0^4 + (c^2 - r_0^2)/(c^2 + r_0^2)^2 \right]}, \\
\gamma &= \frac{-2L_z^2/r_0^5 + r_0(r_0^2 - 3c^2)/3(c^2 + r_0^2)^3}{3L_z^2/r_0^4 + (c^2 - r_0^2)/(c^2 + r_0^2)^2}.
\end{aligned}
\tag{7}
$$

As one can see, for a given value of $r_0$, $q$ decreases as $\alpha$ increases (see Figure 1). On the other hand, when $\alpha$ is kept constant, $q$ decreases as $r_0$ increases (see Figure 2). Equations (7) give interesting results for small values of $c$. Indeed, for $c \to 0$, we have $\Theta_0 \to 1$, $L_z \to = r_0\Theta_0 \to r_0$, where $\Theta_0$ is the circular velocity. In equations (7), setting $L_z = r_0$ and taking the limits for $c \to 0$, we obtain

$$
A = \frac{2}{r_0}, B = \frac{\alpha}{r_0^2}, q = \left( \frac{2}{\alpha} \right)^{1/2}, \beta = \frac{-\alpha}{2r_0}, \gamma = \frac{-5}{6r_0}. \tag{8}
$$

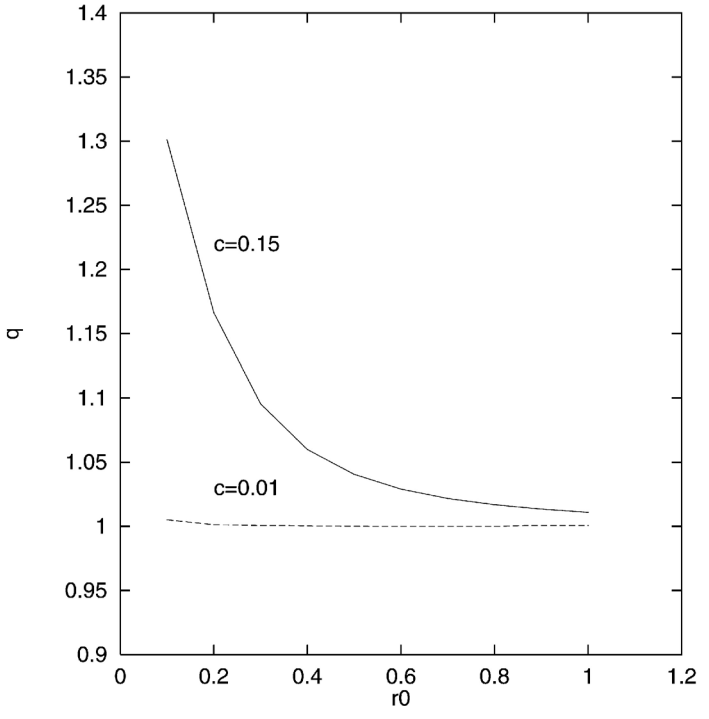


FIGURE 2 Relationship between $q$ and the position of the circular periodic orbit $r_0$. Note that the system shows a quite different behaviour for large values of $c$.

One observes that, for small values of $c$, $q$ is only a function of the flattening parameter $\alpha$ (see Figure 2), while the coefficients $\beta$ and $\gamma$ of the perturbing terms are always negative.

When $\alpha = 1$, potential (2) is spherically symmetric and all three components of the angular momentum are conserved. The corresponding effective potential is

$$V_{\text{eff}}(\rho) = \frac{L^2}{2\rho^2} + \tfrac{1}{2}\ln(\rho^2 + c^2) = \frac{L^2}{2\rho^2} + U(\rho), \tag{9}$$

where $\rho^2 = x^2 + y^2 + z^2$ while

$$L^2 = L_x^2 + L_y^2 + L_z^2 \tag{10}$$

is the square of the total angular momentum. The global potential (9) is integrable. Expanding the potential (9) in the vicinity of the circular orbit $\rho = \rho_0$, we find that

$$V(\rho) = \tfrac{1}{2}A_1\rho^2 + \gamma_1\rho^3, \tag{11}$$

where

$$A_1 = \frac{3L^2}{\rho_0^4} + \frac{c^2 - \rho_0^2}{(c^2 + \rho_0^2)^2}, \quad \gamma_1 = \frac{-2L^2}{\rho_0^5} + \frac{\rho_0(\rho_0^2 - 3c^2)}{3(c^2 + \rho_0^2)^3}, \tag{12}$$

where the higher-order terms have been omitted. Clearly the local potential (12) is also integrable.

## 3 PROPERTIES OF MOTION IN THE LOCAL POTENTIAL

The properties of global motion in the potential (2) have been studied by Karanis and Caranicolas (2001). In what follows, the properties of the local motion described by the potential (6) are studied. We now connect some physical properties such as the energy and axial ratio of the equipotential curves of the global and local potentials.

First, the global energy $E$, associated with the potential $V_{\text{eff}}$, is connected to the local energy $h$, associated with the potential $V(x, y)$. It is clear that $E_{00} = V_{\text{eff}}(r_0, 0)$ is the energy of the circular orbit of a radius $r_0$. The energy $E_0 = V_{\text{eff}}(r_0 + \Delta r, \Delta z)$ is the energy in the vicinity of the circular orbit. In other words, $E_{00} =$ constant represents a point in the $r$–$z$ plane, while $E_0 =$ constant represents a curve defining an area in the same plane. The motion takes place inside this curve, usually called the equipotential curve or the curve of zero velocity. The difference $E_0 - E_{00}$ defines the local energy. In order to avoid large numbers, we have divided all parameters by $A$. Thus $h = (E_0 - E_{00})/A$. On increasing $\Delta r$ and $\Delta z$, $E_0$ increases, so that $h$ also increases.

It is interesting to compare the equipotential curves of the logarithmic potential (2) with those of the local potential (6). The axial ratio of the equipotential ellipses for the potential (2) is $a/b = \alpha$ while the axial ratio of the equipotential curves of the local potential (6), which for small values of $h$ can be considered as ellipses, is $a/b = A^{1/2}/B^{1/2} = q$. This is reasonable because the axial ratio of the local potential depends not only on the flattening parameter but also on $c$, $L_z$ and the position $r_0$ of the circular orbit. The axial ratio can be considered to be the same for $\gamma = 0$ or for $\gamma \neq 0$ for low local energies. For higher energies the axial ratio cannot be defined because the zero-velocity curves are not ellipses.

The Hamiltonian for the potential (6) is

$$H = \tfrac{1}{2}\,(p_x^2 + p_y^2 + x^2 + \omega^2 y^2) + \beta x y^2 + \gamma x^3 = h, \tag{13}$$

where $p_x$ and $p_y$ are the momenta per unit mass conjugate to $x$ and $y$ respectively, while $h$ is the numerical value of $H$. In order to visualize the properties of motion in the local potential, we computed the $x$–$p_x (y = 0,\ p_y > 0)$ Poincaré phase plane, for the Hamiltonian (13) in the 1:1 and 4:3 resonance cases. To keep matters simple, only bounded local motion is considered. This means that zero-velocity curves $V(x, y) = h$ are always closed in the $x$–$y$ plane, that is $h < h_{\text{esc}}$, where $h_{\text{esc}}$ is the energy of escape (Caranicolas and Varvoglis, 1984) and is given by

$$h_{\text{esc}} = \frac{1}{54\gamma^2}. \tag{14}$$

When $r_0 = 0.6$, $\alpha = 2$ and $c = 0.01$, we find that $\omega^2 = 1$, $\beta = -1.67$ and $\gamma = -1.39$. The numerical results do not show resonance phenomena for all values of the local energy up to $h_{\text{esc}}$. All invariant curves are topological circles around a stable invariant point. In other words, the local phase plane appears similar to the global $r$–$p_r$ phase plane, in the case where the angular momentum in the effective potential is the circular angular momentum (see Figure 5 later). Similar results are observed when the local system is near the 4:3 resonance. This happens when $r_0 = 0.6$, $\alpha = 1.2$ and $c = 0.15$. The corresponding local parameters are $\omega^2 = 0.56$, $\beta = -0.88$ and $\gamma = -1.38$. The situation appears quite different if we consider only the first coupling perturbing term in the local potential (6). In this case, the last term in equation (6) is neglected (Caranicolas and Innanen, 1992). For convenience, we call this potential $V_{\text{C}}$. Figures 3(a)–(d) show the $x$–$p_x$ Poincaré phase plane for the above values of the parameters and four values of the local energy $h = 0.01$, 0.03 and 0.04 and also $h = h_{\text{Cesc}} = 0.0448$. The pattern has the characteristics of the 1:1 resonance. The motion is regular for small energies

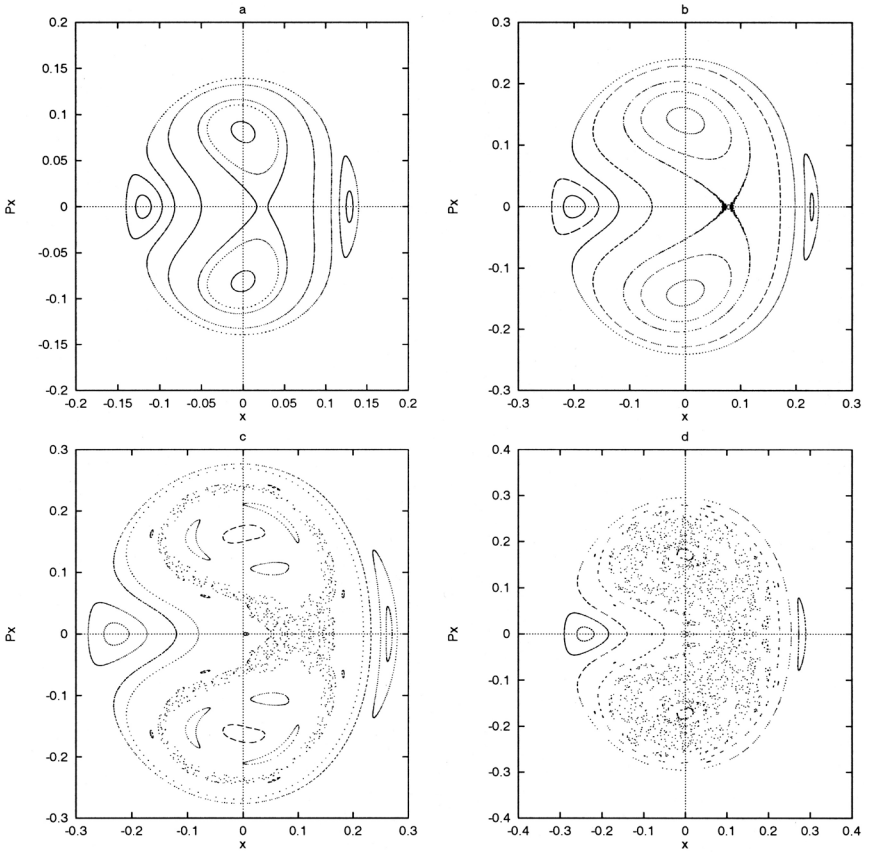


FIGURE 3 (a)–(d) The $x$–$p_x$ phase plane for the local potential $V_C$ in the 1:1 resonance case. Note that resonance phenomena are present for low energies, while the chaotic region increases for higher energies.

while, for $h = 0.03$, a small chaotic layer appears near the separatrix. For $h = 0.04$, the chaotic layer increases and secondary resonances appear while, for $h = h_{esc}$, there exists a chaotic sea and small regular regions around the stable periodic points on the $x$ axis. A similar behaviour is observed in the case when the local system is near the 4:3 resonance. Note that the escape energy for the potential $V_C$ is

$$h_{Cesc} = \frac{\omega^4}{8\beta^2} = \frac{1}{8q^4\beta^2}. \tag{15}$$

The escape energy for the potential $V_C$ depends on the values of $q$ and $\beta$, while the corresponding escape energy for potential (6) depends only on the local parameter $\gamma$.

One could claim that all the above are characteristics of the logarithmic potential (2) and that the behaviours of the local potentials $V$ and $V_C$ could have been different if we had chosen a different global potential. For this reason, we obtained the local potentials corresponding to a composite mass model (CMM) composed of a disc halo, a nucleus, a bulge and a dark halo. The parameters of this model and the corresponding effective potential can be found in the paper by Caranicolas (1997). To help the reader to follow our reasoning, this CMM is described in Appendix A. Figure 4 shows a plot of $q$ as a function the position $r_0$ of the circular periodic orbit in the CMM. As one can see, the system can be, among others, near the 1:1, 1:2, 2:5 and

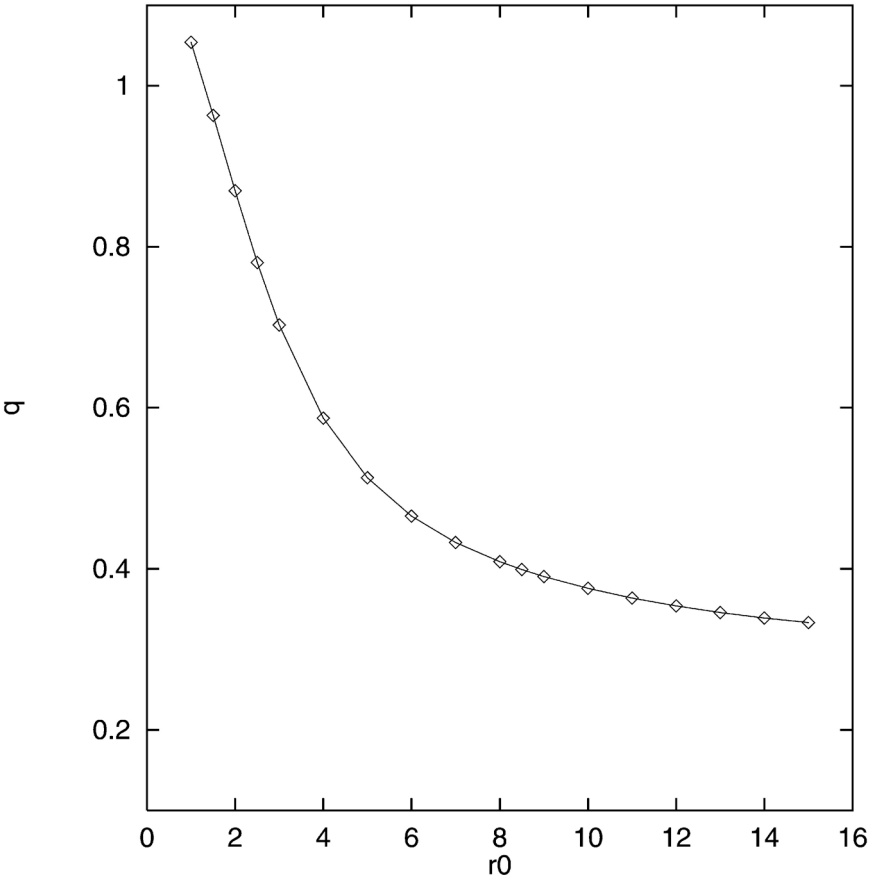


FIGURE 4 Relationship between $q$ and the position of the circular periodic orbit $r_0$ in the local expansion of the CMM. We observe that the system can show a large number of resonances.

1:3 resonance cases. So that the reader can obtain a better view of the local parameters we give the corresponding values for the CMM in Table 1.

Figure 5 shows the $r$–$p_r(z = 0, p_z > 0)$ phase plane in the CMM. The value of angular momentum $L_z$ is equal to $L_{z\text{cir}} = 116$, which is the value of the circular angular momentum at $r_0 = 5.25$. The energy is $E_0 = -1213$, a value which is about 2% higher than the energy $E_{00} = -1242$ of the corresponding circular orbit. This energy defines a zero-velocity curve in the $r$–$z$ plane between $r_{\max} = 6.76$ and $r_{\min} = 4.21$. Figure 5 suggests that there are no resonant phenomena. Here we emphasize that resonance phenomena and chaos, in some global

TABLE 1 Parameters for the local potentials $V$ and $V_C$ derived from the Taylor series of the the CMM.

| $r_0$ | $\omega^2$ | $\beta$ | $\gamma$ | $q$ |
|---|---|---|---|---|
| 1.30 | 1.0 | −0.48 | −0.61 | 1.0 |
| 5.25 | 4.0 | −0.28 | −0.15 | 0.5 |
| 8.50 | 6.27 | −0.46 | −0.10 | 0.4 |
| 15.0 | 9.0 | −0.61 | −0.06 | 0.33 |

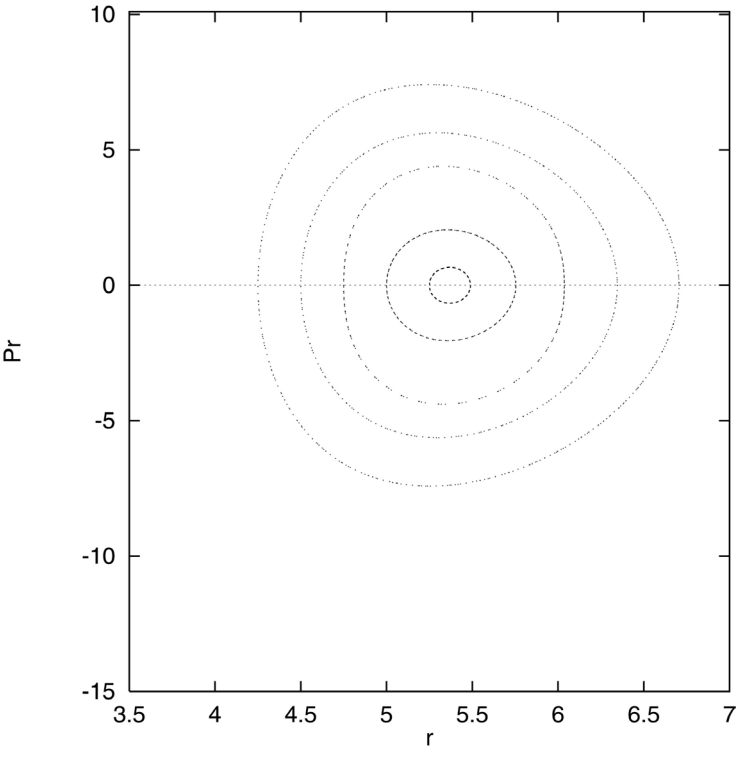


FIGURE 5 The $r$–$p_r$ phase plane for the CMM. The value of the angular momentum $L_{z\mathrm{cir}} = 116$, while $E = E_0 = -1213$. No resonance phenomena are present.

potentials, were observed only for low values of the angular momentum (Caranicolas and Innanen, 1991; Caranicolas, 1997; Karanis and Caranicolas, 2001).

Figures 6(a)–(d) show the $x$–$p_x$ phase plane for the local potentials $V$ and $V_{\mathrm{C}}$ in the case $q = 0.5$ in Table 1. It is clear that the local system is in 1:2 resonance. In Figure 6(a), the $x$–$p_x$ phase plane is shown for the potential $V$ when $h = h_{\mathrm{esc}} = 0.8230$. No resonance phenomena are present. Figure 6(b) shows the $x$–$p_x$ phase plane of the local potential $V_{\mathrm{C}}$ for the same value of $h = 0.8230$. Once again, no resonance phenomena are observed. In order to observe resonance phenomena in the local potential $V_{\mathrm{C}}$, one must go close to $h_{\mathrm{Cesc}}$. Figures 6(c) and (d) show the $x - p_x$ phase plane for this potential when $h = 24.5$ and $h = h_{\mathrm{esc}} = 25.51$, respectively, where resonance islands and chaos are present.

Extensive numerical calculations, in the local potentials $V$ and $V_{\mathrm{C}}$, derived from the logarithmic potential or the CMM, when $q = 1$ or $q = 1.33$ in the first case, and for all values of $q$ shown in Table 1 in the second case, suggest that the potential $V$ does not display resonance phenomena for all values of the energy $h < h_{\mathrm{esc}}$. On the other hand, the potential $V_{\mathrm{C}}$ always displays resonance phenomena. Those phenomena appear for very low energies and are present up to $h = h_{\mathrm{Cesc}}$ when $q = 1$, that is in the 1:1 resonance case, while, for the other resonance cases, they appear only when the energy $h$ of the system is close to $h_{\mathrm{esc}}$.

The above phenomena support the idea that there is a threshold for the parameters of the local system to describe successfully the properties of motion of the global system. Such a parameter is the energy of escape of the local system, which is connected, through equations (14), (15) and (7) to the parameters of the global potential. Up to this energy, the orbital behaviour of the local potential $V$ is similar to that of the global potential (2). For resonance cases different from the 1:1 resonance, the motion in the local potential $V_{\mathrm{C}}$ is similar to the global motion for low local energies, far from the escape energy.

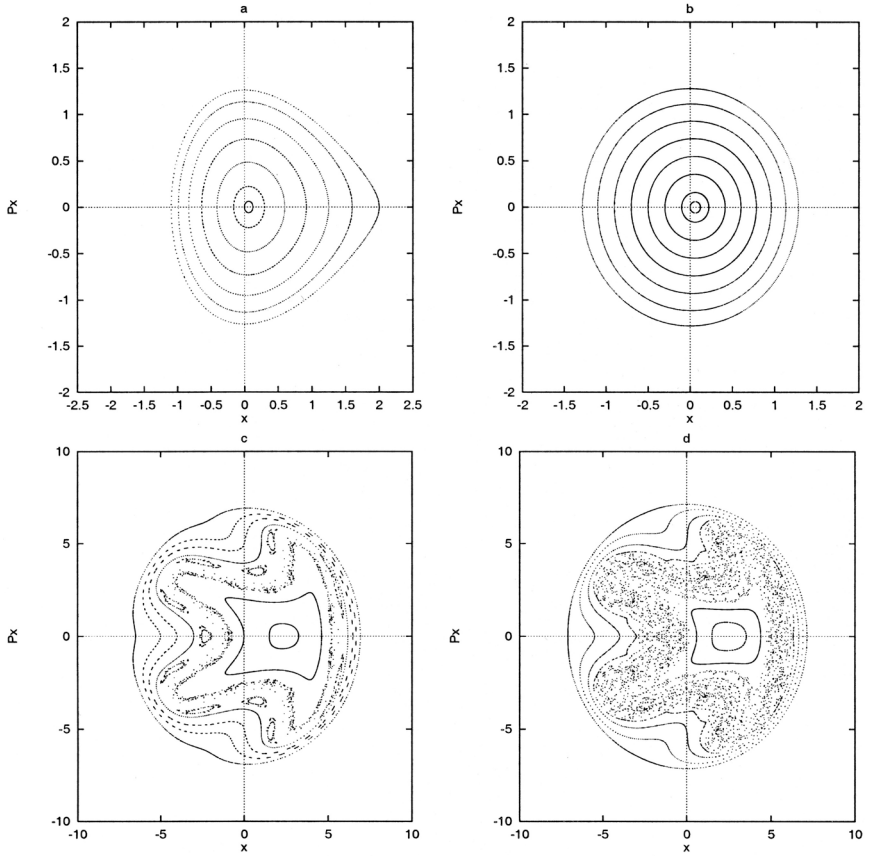


FIGURE 6 The $x$–$p_x$ phase plane for the local potentials (a) $V$ and (b)–(d) $V_C$ in the 1:2 resonance case. Note that no resonance phenomena appear in $V$ while resonance phenomena and chaos appear in $V_C$ only for values of the local energy near $h_{Cesc}$.

## 4 DISCUSSION

In this paper we have tried to connect the parameters of local motion with physical quantities in the global models. Such parameters for the global models used in this work are, among others, the mass, angular momentum, the scale size of the nucleus or bulge and the flattening parameter. In other words, the parameters $\omega, \beta, \gamma$ and the energy $h$ are not arbitrary but are functions of the above physical quantities of the global models.

Two global models were used: the logarithmic potential (2) and the CMM. In the local potential derived from the logarithmic model, two resonance cases are possible: the 1:1 and the 4:3 resonance. In the CMM (Figure 4), a large number of resonance cases are possible. The parameters of the local potential for some of the resonance cases are given in Table 1.

Numerical calculations were carried out in the local potentials $V$ and $V_C$ in the cases where $q = 1/\omega$ was a rational number. In all the studied cases, it was observed that the potential $V_C$ shows resonant phenomena and chaos, while the potential $V$ behaves as if as it was far from resonances even though $q$ is rational. It seems natural then to ask: what is the reason for the different behaviours of the above two local potentials? The answer can be found by observing carefully the patterns given in Figures 5 and 6(a). The similarity between the two patterns is clear. The same behaviours are observed for all values of $q$ in both global potentials. We now

give an explanation for this behaviour. In Figure 5, the properties of global motion for a value of energy $E = E_0$ close to the energy of circular orbit, and a value of the angular momentum corresponding to that of the circular orbit are shown. As the expansion for the potential $V$ is carried to the vicinity of the circular orbit, it is reasonable to expect local motion similar to global motion. Furthermore, if we consider as a value of the local energy that of Figure 6(a), then $h_{\rm esc} = 0.8230 = (E - E_{00})/A$, which for $A = 39$ and $E_{00} = -1242$ gives $E = -1210$. This means that the escape energy of the local system corresponds to an energy $E$ very close to that of the circular orbit. Elementary calculations for the global potential (2) show that $\gamma$ cannot be equal to zero. Indeed, the circular angular momentum is

$$L_z = \frac{r_0^2}{(c^2 + r_0^2)^{1/2}} \tag{16}$$

Substituting this value of $L_z$ in equation (7) for $\gamma$ turns it into a function of $r_0$ and $c$. If $\gamma = 0$, we find only imaginary values for $r_0$, meaning that $\gamma \neq 0$.

On the other hand, in the potential $V_{\rm C}$, we did not take into consideration all third-order terms. As a consequence, one loses information on going from the global to the local potential. Note that, if the term $\gamma$ is ignored at the same time, then all the information coming from the angular momentum in the perturbing terms is lost. This happens because $\beta$ in fact does not depend on the value of the angular momentum while $\gamma$ does depend on this value. This changes drastically the behaviour of the global system. At the same time, this can be considered as a very good example that shows the physical implication resulting from arbitrarily ignoring the term depending on an important physical quantity, that is the angular momentum.

Going a step further, we can state that the resonance phenomena are a consequence of the perturbing terms. If the value of the circular angular momentum is not present in the perturbing terms, then the system displays resonance phenomena. This is reminiscent of the chaotic phenomena in the global motion appearing in both global models for small values of the angular momentum (Caranicolas, 1997; Karanis and Caranicolas, 2001).

The resonance phenomena in the potential $V_{\rm C}$ are stronger and appear for low energies in the 1:1 resonance case while, for other resonance cases, energies near $h_{\rm esc}$ are required to observe them. For low energies, resonance phenomena are not seen. This cannot be considered a better agreement between global and local motion, because we know that in higher-order resonances there are smaller islands and, for resonance phenomena to appear, higher energies are required. Furthermore, the presence of the term $\gamma$ affects the escape energy because it was observed that in all cases $h_{\rm esc} < h_{\rm Cesc}$. It is, therefore, evident that, ignoring $\gamma$, we change the dynamics of the local potential because, among others, we increase the local escape energy, which favours the presence of the reasonance phenomena.

In conclusion, the properties of local motion, in the two global models considered above, are well described by the potential $V$ but not by the potential $V_{\rm C}$. On the other hand, the potential $V_{\rm C}$ is very useful in order to study the properties of perturbed harmonic oscillators, while $V$ does not seem to give interesting results for the same purpose unless we choose arbitrary values for the parameters $\beta$ and $\gamma$. As a related case, we mention the Henon–Heiles (1964) potential where $\beta = 1$ and $\gamma = -1/3$ were chosen after some trials. The complex sensitivities of its parameters for the onset of chaos have been studied by Innanen (1985). Future studies aim to examine the theoretical effects produced by perturbations of galactic bars and/or other non-axisymmetric mass distributions.

***Acknowledgements***

The author would like to thank Professor K.A. Innanen and Professor N.K. Spyrou for their useful suggestions and comments.

### *References*

Binney, J., and Tremaine, Sc. (1987) *Galatic Dynamics*, Princeton University Press, Princeton, New Jersey.
Caranicolas, N.D. (1989) *J. Astron. Astrophys.* **10**, 197.
Caranicolas, N.D. (1990) *Celestial Mech.* **47**, 87.
Caranicolas, N.D. (1997) *Astrophys. Space Sci.* **246**, 15.
Caranicolas, N.D., and Innanen, K.A. (1991) *Astron. J.* **102**, 1343.
Caranicolas, N.D., and Innanen, K.A. (1992) *Astron. J.* **103**, 1308.
Caranicolas, N.D., and Varvoglis, H. (1984) *Astron. Astrophys.* **141**, 383.
Caranicolas, N.D., and Vozikis, Ch. (1986) *Celestial Mech.* **39**, 105.
Elipe, A., Miller, B., and Vallejo, M. (1995) *Astron. Astrophys.* **300**, 722.
Henon, M., and Heiles, C. (1964) *Astron. J.* **69**, 73.
Innanen, K.A. (1985) *Astron. J.* **90**, 2377.
Karanis, G.I., and Caranicolas, N.D. (2001) *Astron. Astrophys.* **367**, 443.
Richstone, D. (1980) *Astrophys. J.* **238**, 103.
Richstone, D. (1982) *Astrophys. J.* **252,** 496.
Saito, N., and Ichimura, A. (1974) In: Casati, G. and Ford, J. (eds.), *Stochastic Behaviour in Classical and Quantum Hamiltonian Systems*, Springer, Berlin, p. 137.

## APPENDIX A

### A1 The composite mass model

We consider an axially symmetric galaxy model consisting of four components, in the same way as in the paper by Caranicolas and Innanen (1991). The first component is the disc-halo represented by the potential

$$\Phi_{\rm dh} = -\frac{M_{\rm dh}}{R}, \tag{A1}$$

with

$$R^2 = \left(k + \sum_{i=1}^{3} \lambda_i (z^2 + h_i^2)^{1/2}\right)^2 + d^2 + r^2. \tag{A2}$$

Here $r$ and $z$ are the traditional galatic cylindrical coordinates, $M_{\rm dh}$ is the mass, $k$ and $h$ are the scale length and the scale height of the disc respectively, while $d$ is the core radius scale length of the halo component. $\lambda_1$, $\lambda_2$ and $\lambda_3$ represent the fractional portions of the old disc, dark matter and young disc respectively. The other three components are represented by the spherically symmetric potentials

$$\begin{aligned}
\Phi_{\rm n} &= -\frac{M_{\rm n}}{(r^2 + z^2 + c_{\rm n}^2)^{1/2}}, \\
\Phi_{\rm b} &= -\frac{M_{\rm b}}{(r^2 + z^2 + c_{\rm b}^2)^{1/2}}, \\
\Phi_{\rm h} &= -\frac{M_{\rm h}}{(r^2 + z^2 + c_{\rm h}^2)^{1/2}},
\end{aligned} \tag{A3}$$

where $M_{\rm n}$, $M_{\rm b}$ and $M_{\rm h}$, are the masses of the nucleus, bulge and dark halo respectively, and $c_{\rm n}$, $c_{\rm b}$ and $c_{\rm h}$ are their corresponding scale lengths.

We use a system of galatic units where the unit of length is 1 kpc, the unit of mass is $2.325 \times 10^7 M$ and the unit of time is $0.977\,748 \times 10^8$ year. The velocity unit is $10\,{\rm km\,s^{-1}}$ while $G = 1$. Using these units, we take $M_{\rm dh} = 9350$, $M_{\rm n} = 400$, $M_{\rm b} = 2000$, $M_{\rm h} = 11\,500$, $k = 3.1\,{\rm kpc}$, $d = 10\,{\rm kpc}$, $\lambda_1 = 0.4$, $\lambda_2 = 0.5$, $\lambda_3 = 0.1$, $h_1 = 0.325\,{\rm kpc}$, $h_2 = 0.090\,{\rm kpc}$, $h_3 = 0.125\,{\rm kpc}$, $c_{\rm h} = 0.25\,{\rm kpc}$, $c_{\rm b} = 3\,{\rm kpc}$ and $c_{\rm h} = 40\,{\rm kpc}$. This choice of units produces a composite galactic mass model that reasonably replicates our Galaxy, with a flat rotation curve.